International Journal of Electrical, Electronic and Communication Sciences
ISSN: 2517-9438
Vol:11, No:6, 2017

Development and Validation of Cylindrical Linear Oscillating Generator

Sungin Jeong

***Abstract*—**This paper presents a linear oscillating generator of cylindrical type for hybrid electric vehicle application. The focus of the study is the suggestion of the optimal model and the design rule of the cylindrical linear oscillating generator with permanent magnet in the back-iron translator. The cylindrical topology is achieved using equivalent magnetic circuit considering leakage elements as initial modeling. This topology with permanent magnet in the back-iron translator is described by number of phases and displacement of stroke. For more accurate analysis of an oscillating machine, it will be compared by moving just one-pole pitch forward and backward the thrust of single-phase system and three-phase system. Through the analysis and comparison, a single-phase system of cylindrical topology as the optimal topology is selected. Finally, the detailed design of the optimal topology takes the magnetic saturation effects into account by finite element analysis. Besides, the losses are examined to obtain more accurate results; copper loss in the conductors of machine windings, eddy-current loss of permanent magnet, and iron-loss of specific material of electrical steel. The considerations of thermal performances and mechanical robustness are essential, because they have an effect on the entire efficiency and the insulations of the machine due to the losses of the high temperature generated in each region of the generator. Besides electric machine with linear oscillating movement requires a support system that can resist dynamic forces and mechanical masses. As a result, the fatigue analysis of shaft is achieved by the kinetic equations. Also, the thermal characteristics are analyzed by the operating frequency in each region. The results of this study will give a very important design rule in the design of linear oscillating machines. It enables us to more accurate machine design and more accurate prediction of machine performances.

***Keywords*—**Equivalent magnetic circuit, finite element analysis, hybrid electric vehicle, free piston engine, cylindrical linear oscillating generator

I. Introduction

AN electrical machine as energy converter has been getting into the spotlight in the province of hybrid electric vehicle (HEV). HEV taking advantages of the oscillating motion is a good solution to the problems of energy crisis and environmental pollution nowadays on account of various modularity and optimal energy utilization. In electrical machines of continuous motion conversion of energy from mechanical to electrical results from effect of action of the constant component of force in case of linear motion. These linear oscillating machines have many advantages because of the possibility of direct connection between moveable part and oscillating working body of driven mechanism without mechanical components such as drive rod, crank shaft, and crank gear. So, the principle of direct drive could be accomplished. The linear oscillating generators could be applied to the same benefit driven by free piston engines. In this case of the mover of generator can be directly connected with the oscillating engine piston (or piston). A linear oscillating generator converts the mover's kinetic energy directly to electric energy without additional mechanical apparatus. As a result, it enables to higher efficiency and lower manufacturing expense, therefore the linear oscillating generator has a potential energy for use in a series hybrid electric vehicle power train. Moreover, the free piston motion can be used by using linear oscillating principles [1]. Meanwhile, test results of some prototype equipment with linear internal combustion engines have been published. But a comprehensive study of linear oscillating generators is still missing. Especially questions concerning the number of phases, excitation method, bearing construction, voltage stability under load, sensor and inverter equipment are not satisfied answered. This paper deals with the investigation and assessment of different systems and some kinds of category in terms of:

- Power to weight and volume ratio,
- Efficiency,
- Reactive power consumption.

The cylindrical topology will be achieved by Equivalent Magnetic Circuit Network (EMCN) method. The analysis of the topology considering leakage reluctance is compared to the result of Finite Element (FE) method by static magnetic field, and then the optimal model will be selected by characteristics and results through the number of phases by displaement of the stroke. Finally, this topology will be approached through detailed design taking nonlinear properties of iron-core into account [1]. Besides, the thermal and shaft robustness characteristics take into account by operating frequency and fatigue limit to ensure the operating temperatures do not exceed the acceptable limits of used material and resist dynamic forces and the resulting vibrations, respectively.

The first step will be the development of analytical design data for the different phase systems of cylindrical topology and the checking of the design by numerical field calculations and thermal calculations. In addition, shaft design will be performed considering acceleration force by load mass because the shaft is seriously affected by bending and axial loads. The optimum topology will be manufactured and experimented by the simulation analysis considering nonlinear effects of combustion process. It enable to complete the knowledge about operational behavior of the machine and inverter. At last its assessment has to be elaborated and will give useful information and potential for the performance advancement.

Sungin Jeong is with the R&D Center, Daelim Motor, Republic of Korea (e-mail: in8130@hanyang.ac.kr).

II. Analysis Procedure

In preliminary analytical design methodologies, the approaches by prediction or experience of the behavior of electric machines by designer have been used. However, this process for the analysis and design of the machines have been overlooked or compensated by correction factors for the accurate flux saturation. Therefore, this paper investigates the machine dimensioning with help of the EMCN as initial design process. By comparison and analysis of the number of phases by scientific backgrounds, the optimal model is selected. The optimal system will be designed in detail taking saturation into account by FE analysis. For accurate and complete design, the shaft and thermal analysis is also calculated. When designing an electrical machine, it is important to consider magnetic saturation in magnetic steel as it will increase losses and decrease machine performance [1]. Therefore, it is generally used for initial design, and confirmation or modification using other approaches (e.g., FE method) is required. The FE analysis is one of the most commonly used methods for analysis of electric machines nowadays [1], [2].

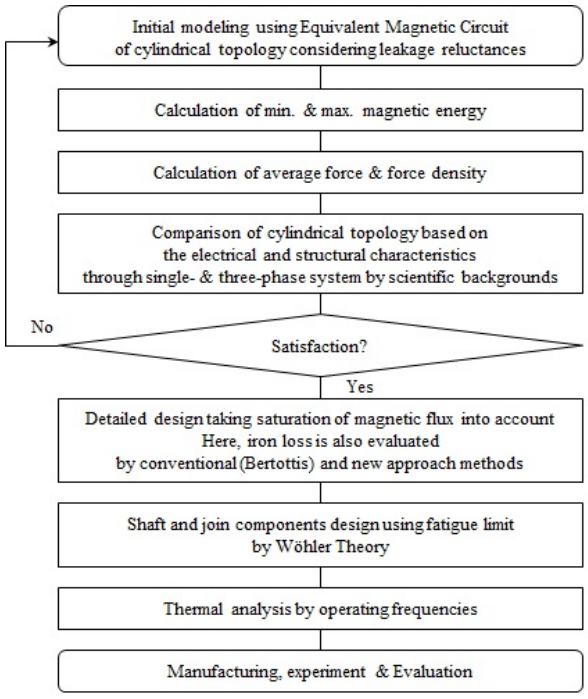

Fig. 1 Analysis Flow

III. Cylindrical Topology

Among the various linear generators, cylindrical topology with magnet excitation are particularly popular, since they hardly experience typical assembly problems of linear machines; conforming to a compact structure and a low weight compared with the force. The cylindrical type linear generator includes an armature and a translator. The former consists of a single conductive wire cylindrically wound and encapsulated, while the latter is a cylindrical assembly of sintered NdFeB permanent magnets arrayed at an axial North-South stack contained in an encasing tube. Recently, cylindrical linear permanent magnet machine became an attractive candidate for servo systems in need of high precision control, in spite of such disadvantages as difficulty of manufacturing of a magnet mover, maintaining fixed air-gap length and laminating for reduced eddy-current loss. Moreover, linear oscillating generator with tubular configuration has advantages of exhibiting high force to volume ratios and high positioning speed. The rotation of the piston has not a bad influence on the electric characteristics of the linear oscillating generator [2]. The cylindrical type linear generator has some more advantages than flat type one as following aspects; it has higher efficiency, reliability and leakage is smaller because of its symmetric structural merits. Also, the amount of copper is less because no winding overhang is required, therefore the copper loss becomes less than that of flat type linear generator. The shaft is cylindrical and it can be easily connected with the rod of the engine piston without complex mechanical structure. Furthermore, the cylindrical translator can be rotated freely with the piston of the engine and there is no interference to the magnetic characteristics in the linear generator. From now on, it deals with characteristics and analysis by number of phases through the proposed new structure.

A. Analytical Calculation

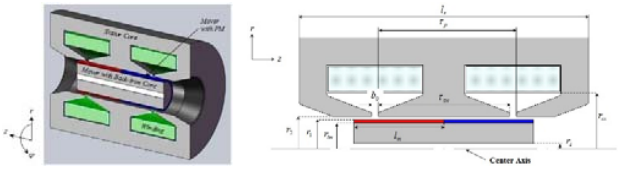

3- Dimension 2-Dimension

Fig. 2 Cylindrical Topology

There is the dimension for the analytical calculation of reluctances and the winding circuit of single-phase system in Fig. 2. Predefined formulation for the reluctance calculation is described by (1) ~ (4):

$$\Theta_a = N_c \cdot I \tag{1}$$

$$\Theta_m = \frac{B_{rem} \cdot (r_1 - r_{im})}{\mu_0 \cdot \mu_r} \tag{2}$$

$$R_\delta = \frac{1}{\mu_0} \cdot \frac{\delta}{2 \cdot \pi \cdot (r_2 - r_1) \cdot \tau_{sw}} \tag{3}$$

$$R_m = \frac{1}{\mu_0 \cdot \mu_r} \cdot \frac{r_1 - r_{im}}{2 \cdot \pi \cdot (r_1 - r_{im}) \cdot l_m} \tag{4}$$

where number of windings N_c, input current I, residual magnetic flux density B_{rem}, and length of air-gap δ. Also, R_δ and R_m represents the reluctance at air-gap and magnet, respectively.

1. Maximum Magnetic Energy

To correctly estimate the reluctance variation, it is necessary to model a reasonable formulation of the various reluctances (permeances) of the machines. Now, the characteristic of the

maximum magnetic energy can be calculated by equivalent circuit at unaligned position as shown Fig. 3.

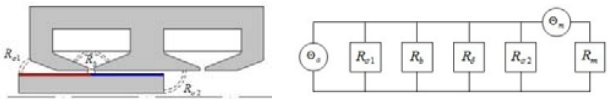

Fig. 3 Maximum Position

In the unaligned position, reluctances are divided into three parts; $R_{\sigma 1}$, $R_{\sigma 2}$ and R_b. They express the leakage reluctance of left-side, right-side and interactive fringing reluctance between permanent magnet poles and end part of the armature tooth in the slot-opening, respectively.

$$R_{\sigma 1} = \frac{1}{\mu_0}\cdot\frac{\delta}{2\cdot\pi\cdot(r_2-r_1)\cdot\left(l_m-\frac{\tau_{sw}}{2}\right)}+\frac{1}{\mu_0}\cdot\frac{\pi}{9}\cdot\frac{1}{2\cdot\pi\cdot(r_2-r_1)}\cdot\frac{1}{\ln\left(\frac{l_m-\frac{\tau_{sw}}{2}}{\delta}\right)} \quad (5)$$

$$R_{\sigma 2} = \frac{1}{\mu_0}\cdot\frac{\delta}{2\cdot\pi\cdot(r_2-r_1)\cdot(r_{im}-r_s)}+\frac{1}{\mu_0}\cdot\frac{\pi}{2}\cdot\frac{1}{2\cdot\pi\cdot(r_2-r_1)}\cdot\frac{1}{\ln\left(\frac{r_{im}-r_s}{r_1-r_{im}}\right)} \quad (6)$$

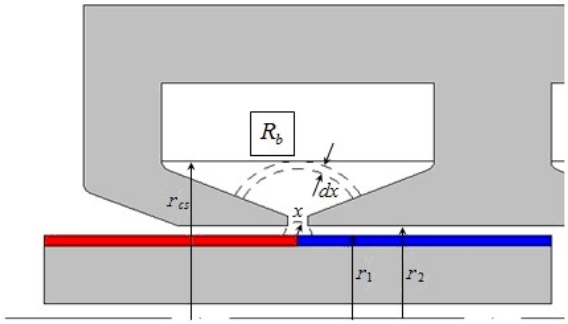

Fig. 4 Permeance at Maximum Position

Magnifying region R_b of the Fig. 4, it is as shown in Fig. 3 and represents fringing permeance in (7):

$$P_b = \sum\frac{\mu_0\cdot 2\pi\cdot(r_{cs}-r_2)\cdot dx}{b_0+\pi\cdot x} = \int_{r_1}^{r_{cs}}\frac{\mu_0\cdot 2\pi\cdot(r_{cs}-r_2)}{b_0+\pi\cdot x}\cdot dx = \frac{\mu_0\cdot 2\pi\cdot(r_{cs}-r_2)}{\pi}\cdot\ln\left(1+\frac{\pi\cdot(r_{cs}-r_1)}{b_0}\right) \quad (7)$$

To obtain the minimum magnetic energy, it should be solved of the reluctance network matrix using the above reluctance formulas.

$$\begin{bmatrix}\phi_1\\ \phi_2\\ \phi_3\\ \phi_4\\ \phi_5\end{bmatrix} = \begin{bmatrix} R_{\sigma 1} & -R_{\sigma 1} & 0 & 0 & 0\\ -R_{\sigma 1} & R_{\sigma 1}+R_b & -R_b & 0 & 0\\ 0 & -R_b & R_b+R_\delta & -R_\delta & 0\\ 0 & 0 & -R_\delta & R_\delta+R_{\sigma 2} & -R_{\sigma 2}\\ 0 & 0 & 0 & -R_{\sigma 2} & R_{\sigma 2}+R_m\end{bmatrix}^{-1}\cdot\begin{bmatrix}\Theta_a\\ 0\\ 0\\ 0\\ \Theta_m\end{bmatrix} \quad (8)$$

2. Minimum Magnetic Energy

An average force can be calculated by gradient between maximum and minimum of magnetic energy. The magnetic energy has a minimum value at the aligned position; it consists of the $R_{\sigma 3}$ and R_{ns} as shown in Fig. 5.

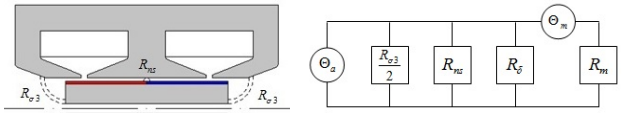

Fig. 5 Minimum Position

Under the aligned position, the leakage reluctance at the both ends can be expressed by (9):

$$R_{\sigma 3} = \frac{1}{\mu_0}\cdot\frac{\delta}{2\cdot\pi\cdot(r_2-r_1)\cdot\left(\frac{l_s}{2}-l_m\right)}+\frac{1}{\mu_0}\cdot\left(\frac{\pi}{2}+\frac{\pi}{9}\right)\cdot\frac{1}{2\cdot\pi\cdot(r_2-r_1)}\cdot\frac{1}{\ln\left(\frac{r_{im}-r_s}{r_1-r_{im}}\right)} \quad (9)$$

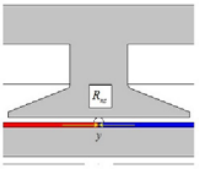

Fig. 6 Permeance at Minimum Position

The R_{ns} indicates the leakage reluctance between armature teeth and two magnet poles in the air-gap. It can be expressed as (10) by Fig. 6:

$$P_{ns} = \sum\frac{\mu_0\cdot 2\pi\cdot(r_2-r_1)\cdot dx}{\lim_{y\to\infty}\frac{1}{y}+\pi\cdot x} = \int_0^{\delta}\frac{\mu_0\cdot 2\pi\cdot(r_2-r_1)}{\lim_{y\to\infty}\frac{1}{y}+\pi\cdot x}\cdot dx = \frac{\mu_0\cdot 2\pi\cdot(r_2-r_1)}{\pi}\cdot\ln\left(1+\frac{\pi\cdot\delta}{\lim_{y\to\infty}\frac{1}{y}}\right) \quad (10)$$

Just like preceding calculation of maximum magnetic energy, the matrix of reluctance network for minimum magnetic energy by Fig. 5 is as:

$$\begin{bmatrix}\phi_6\\ \phi_7\\ \phi_8\\ \phi_9\end{bmatrix} = \begin{bmatrix}\frac{R_{\sigma 3}}{2} & -\frac{R_{\sigma 3}}{2} & 0 & 0\\ -\frac{R_{\sigma 3}}{2} & \frac{R_{\sigma 3}}{2}+R_{ns} & -R_{ns} & 0\\ 0 & -R_{ns} & R_{ns}+R_\delta & -R_\delta\\ 0 & 0 & -R_\delta & R_\delta+R_m\end{bmatrix}^{-1}\cdot\begin{bmatrix}\Theta_a\\ 0\\ 0\\ \Theta_m\end{bmatrix} \quad (11)$$

3. Calculation of Magnetic Energy and Force

The formula for the calculation of the magnetic energy and force is satisfied as:

$$\Delta W = W_{\max}-W_{\min} = \left(\frac{1}{2}\cdot\phi_{\max}^2\cdot R_{\max}\right)-\left(\frac{1}{2}\cdot\phi_{\min}^2\cdot R_{\min}\right) = \frac{1}{2}\cdot\left[\left(\phi_{\max}^2\cdot R_{\max}-\phi_{\min}^2\cdot R_{\min}\right)\right] \quad (12)$$

where, the suffix of each character such as max and min means the magnetic energy, flux linkage and reluctance at the maximum and minimum position, respectively.

$$F_{ave} = \frac{\Delta W}{\tau_p} \quad (13)$$

A magnetic network by Kirchhoff Law can be expressed in analogy through electrical circuit theory. By simply equivalence, the average force and force density is derived by

using difference of maximum and minimum magnetic energy. The flux equations above are obtained by calculating and the equivalent magnetic circuit in aligned (maximum) and unaligned (minimum) position, respectively.

B. Summary

This chapter studied about cylindrical type with single-phase system. The main advantage of cylindrical linear construction arises from its inherent ability to neutralize normal forces acting between the stator and the translator, which enables accomplishment of the design. In addition, the nonexistence of end-turns effect brings about not only minimization of power loss, but also high force per volume ratio. It conduces to favorable generator characteristics. This helps accomplishment to minimize the leakage and to optimize the back iron in mover. The comparison of results between equivalent magnetic circuit analysis and FE method will be continuously achieved in *V. Detailed Design*.

IV. Selection of Optimal System

This chapter contains the electrical characteristic results based on the performances by both EMCN method and FE analysis in the whole models. It examines closely the conformity between the analytical calculation and FE analysis results of the studied topology representing the device as a magnetic circuit (reluctance network). And then, the difference by number of phases is accomplished through the universal and mathematical analysis. At last, cylindrical topology with single-phase is selected for optimal model by comparing the structural features and the characteristics of each phase. In the next step, the topology will be taken with magnetic flux saturation by nonlinear iron property into account. In order to select the optimal topology on the basis of these characteristics, it is also considered by three categories;

- Advantages / Disadvantages of the topology
- Academic difference of single- and three-phase

A. Difference between Single- and Three-Phase

The comparative analysis of single-phase and three-phase system is achieved for the development of oscillating free piston internal combustion engines. It is evaluated in respect of the mathematical difference of continuous motion.

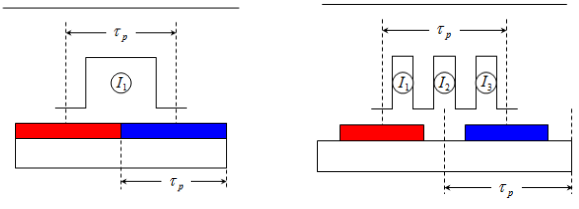

Single-Phase Three-Phase

Fig. 7 Comparison of the Geometric Conditions

As constants, a permanent magnet excitation with trapezoidal spatial flux density distribution is assumed. If we assume a limited motion by one pole pitch only what is typically possible in oscillating machines, the calculation approach for the thrust has to be modified. While in the three-phase system operated on an inverter bridge, the current sheet is more or less sinusoidal, also a magnet width - pole pitch ratio which emphasizes the first harmonic of the flux density distribution ($\alpha \cdot p \doteq 0.72$) is preferable. With the single-phase system, instead a more rectangular flux density distribution is the best approach as the one-phase is operated on a 4 Quadrant chopper which can produce a nearly rectangular current sheet (Fig. 7).

Calculating the inductances from the flux linkage, we find different expressions:

$$\hat{\Psi}^{(1)} = (w_s \cdot \zeta_s)^2 \cdot \frac{1}{2} \cdot \frac{\mu_0 \cdot \tau_p \cdot l_E}{\delta''} \cdot \hat{I}_s \tag{14}$$

$$\hat{\Psi}^{(3)} = (w_s \cdot \zeta_s)^2 \cdot \frac{2}{\pi^2} \cdot m_s \cdot \frac{\mu_0 \cdot \tau_p \cdot l_E}{\delta''} \cdot \hat{I}_s \tag{15}$$

$$\frac{L_h^{(1)}}{L_h^{(3)}} = \frac{1 \cdot \pi^2}{2 \cdot 2 \cdot m_s} = 0.82 \tag{16}$$

The copper losses can be calculated for one slot and one phase with the copper volume, V_{cu};

$$P_{vcu} = J^2 \cdot \frac{V_{cu}}{\kappa} = R_s \cdot I_s^2 \tag{17}$$

with current density J, and conductivity κ. Assuming same losses in both single-phase and three-phase system, we find equal current densities and:

$$V_{cu}^{(1)} = 3 \cdot V_{cu}^{(3)} \text{ as } I_s^{(1)} = 3 \cdot I_s^{(3)} \tag{18}$$

For the voltage, we have two options; We can assume same terminal voltage or same voltage of the intermediate circuit. This depends on application and load of the generator. If we have an automotive application in mind, we have an on-board battery with limited voltage and so in practice we have to compare systems with same intermediate circuit voltage. With the 4 Quadrant chopper and the single-phase system, we have *Root* 3 higher phase voltage than with the 6-pulse bridge inverter. With the absolute value of the voltage and setting the winding factors to unity, we find approximately.

$$|U_s| \approx \omega_s \cdot L_h \cdot I_s \tag{19}$$

$$\left|\frac{U_s^{(1)}}{U_s^{(3)}}\right| = \sqrt{3} = 0.82 \cdot \frac{\left(w_s^{(1)}\right)^2}{\left(w_s^{(3)}\right)^2} \cdot \frac{I_s^{(1)}}{I_s^{(3)}} = 0.82 \cdot \frac{\left(w_s^{(1)}\right)^2}{\left(w_s^{(3)}\right)^2} \cdot 3 \tag{20}$$

$$\frac{\left(w_s^{(1)}\right)^2}{\left(w_s^{(3)}\right)^2} = \frac{\sqrt{3}}{3 \cdot 0.82} = \frac{1}{0.82 \cdot \sqrt{3}} = 0.704 \tag{21}$$

$$\frac{w_s^{(1)}}{w_s^{(3)}} = 0.84 \tag{22}$$

From the winding ratio, we can calculate now the current sheet;

$$\frac{A_s^{(1)}}{A_s^{(3)}} = \frac{w_s^{(1)} \cdot I_s^{(1)}}{m_s \cdot w_s^{(3)} \cdot I_s^{(3)}} = \frac{0.84 \cdot 3}{3 \cdot 1} = 0.84 \quad (23)$$

With the same flux density amplitude, we find the thrust ratio:

$$\frac{\tau_w^{(1)}}{\tau_w^{(3)}} = \frac{B_\delta^{(1)} \cdot A_s^{(1)}}{B_\delta^{(3)} \cdot A_s^{(3)}} = \frac{B_\delta^{(1)}}{\frac{\left(\hat{B}_\delta^{(3)}\right)}{\sqrt{2}}} \cdot \frac{A_s^{(1)}}{A_s^{(3)}} = \frac{0.84}{\frac{1}{\sqrt{2}}} = 1.19 \quad (24)$$

The thrust of a single-phase system can under the assumed circumstances be 19[%] higher than the thrust of a three-phase system.

V. Detailed Design

Accurate modeling of a machine in different methods is employed to carry out the calculation including numerical methods and equivalent magnetic circuit which is a kind of analytical methods. These methods try to find out closed form expressions for magnetic fields in a machine. However, they cannot consider iron saturation which has significant effect on magnetic fields of machines. This is developed and extended in corporation with FE method resulting in very accurate field and force prediction. Finally, it will be discussed about comparison result of the analytical calculations using equivalent magnetic circuit method and influence of the magnetic flux saturation in cylindrical topology by the concrete dimension.

A. Governing Equations

In order to establish an analytical expression for the magnetic field distribution in the cylindrical machine, the following assumption is made: the relative permeability of stator iron is infinite, and the stator windings are replaced by an equivalent current sheet travelling in space and varying in time. This current sheet is located at the stator surface between the stator and the effective air-gap. The magnetic field analysis is confined to two regions, the air / winding region in which the permeability is μ_0, and the permanent magnet region in which the permeability is $\mu_0.\mu_r$. To begin with, it requires consideration about the magnetic field distribution in air-gap region.

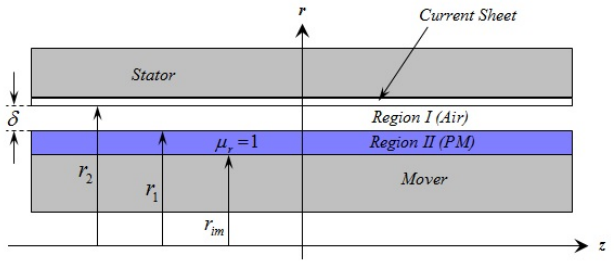

Fig. 8 Analytical Field Model

The partial differential equation for quasi-stationary magnetic fields in continuous and isotropic region can be expressed in terms of the magnetic vector potential A, subject to the Coulomb gauge,

$$\left.\begin{aligned} B &= \mu_0 H \\ \nabla^2 A_I &= 0 \end{aligned}\right\} \quad \text{in the air / winding / iron-core} \quad (25)$$

The flux density components are deduced from A_Θ by:

$$B_z = \frac{1}{r}\frac{\partial}{\partial r}(r A_\theta) \qquad B_r = -\frac{\partial}{\partial z}(A_\theta) \quad (26)$$

Since the field is axially symmetric, A only has the component A_Θ, which is independent of θ.

$$\frac{\partial}{\partial z}\left(\frac{1}{r}\frac{\partial}{\partial z}(r A_{I\theta})\right) + \frac{\partial}{\partial r}\left(\frac{1}{r}\frac{\partial}{\partial r}(r A_{I\theta})\right) = 0 \quad \text{in the air / winding / iron-core} \quad (27)$$

The boundary conditions to be satisfied by the solution to (10.3) are:

$$B_{Iz}\big|_{r=r_2} = 0 \qquad B_{IIz}\big|_{r=r_1} = 0 \quad (28)$$

It can be achieved by the derivation with Maxwell's Equations for quasi-static magnetic fields. The Poisson's equation in 2-D of the machine can be simplified depending on which excitation is present in each particular region.

TABLE I
Governing Partial Differential Equations

Region	μ_r	Equation
Stator-iron	∞	$\nabla^2 \cdot A = 0$
Windings	1	$\nabla^2 \cdot A = -\mu_r \cdot J$
Air-gap	1	$\nabla^2 \cdot A = 0$
Permanent Magnets	μ_r	$\nabla^2 \cdot A = -\nabla \times B_r$
Back-iron in Mover	∞	$\nabla^2 \cdot A = 0$

Through the Fig. 8, Table I shows the governing equation for each region only with the excitation due to the stator current sheet. The equations for stator and air-gap are Laplace equations while for permanent magnets and mover back-iron are Poisson's equations [3]. Equations (29)-(32) represent the flux density:

$$B_{tooth-tip} = \frac{\phi_{tooth-tip}}{\pi \cdot \left\{\left[r_2 + h_t + (t_{hh} - t_h)\right]^2 - r_2^2\right\}} \quad \text{tooth-tip} \quad (29)$$

$$B_{tooth} = \frac{\phi_{tooth}}{2 \cdot \pi \cdot \left[r_2 + h_t + (t_{hh} - t_h) + \frac{t_h}{2}\right]} \cdot l_w \quad \text{tooth} \quad (30)$$

$$B_{yoke} = \frac{\phi_{tooth}}{\pi \cdot [r_o^2 - (r_o - h_{ys})^2]} \quad \text{yoke} \quad (31)$$

$$B_{bi-mover} = \frac{\int_{\frac{b_0}{2} - z_d}^{\frac{b_0}{2} + \tau_{sw} - z_d} 2 \cdot \pi \cdot r_s \cdot B_\delta \, dz}{2\pi \cdot \left(r_{im}^2 - r_s^2\right)} \quad \text{back-iron in the mover} \quad (32)$$

The flux linkage with the stator coil may be obtained by the

following integration. The force generated by Lorentz Law is determined by quantity of the flux in the air-gap and number of turns and circuit in the coil.

$$\phi_\delta = \int_{-\tau_m}^{\tau_m} 2\cdot\pi\cdot r_1\cdot B_\delta \, dz \tag{33}$$

$$F_{orce} = \int_V (J_n \times B) dV = 2\cdot\pi\cdot\Theta\cdot l_m \cdot \frac{\phi_\delta}{(r_1^2 - r_{im}^2)\cdot\pi} \tag{34}$$

where, J_n denotes the current density vector in the winding region, and is expressed in (35):

$$J_n = -\frac{4N_c}{n\pi\tau_p}\sin\left(\frac{n\pi}{2}\right) \tag{35}$$

where, n is the n[th]-order number of the space harmonic. Also, Θ means the magnetomotive force.

B. Comparison Results

Fig. 9 indicates the variety of force characteristics by three kinds of analysis. There are small differences in the average force value between analytical calculation with considering saturation and FE method. It should be noted that the effect of the slot-openings may not be accounted for by slotting factor. Nevertheless, in terms of the average force, all of the preliminary design by EMC and the detailed design considering saturation is within less than 8[%] compared to the FE method result.

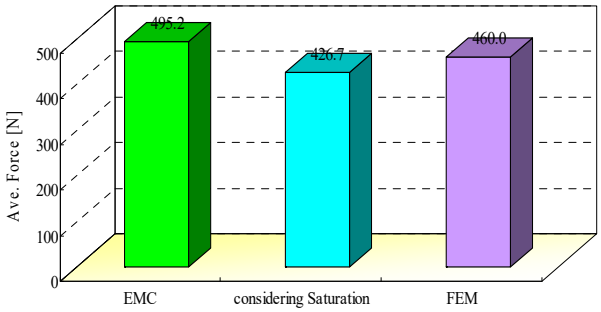

Fig. 9 Comparison of Average Force by Calculation Methods

C. Calculation Losses

As investigated in the previous chapters, a permanent magnet generator of cylindrical linear type with back-iron in the mover can be used especially in hybrid vehicles to power traction drives due to its high force density, wide speed range, and high efficiency. In particular, the back-iron core in this mover structure has a double face; one is the advantage that its establishment causes an efficient flux path, the other is that it leads to the increasing of the material cost due to adding the iron core volume. Therefore, this paragraph will investigate the various losses for the sake of the accurate performance evaluation of the machine; copper loss, eddy-current loss of the permanent magnet and iron loss consisting of hysteresis, eddy current, and excess loss.

First of all, the calculation of the iron loss with the help of the *Steinmetz* equation is still used at high frequencies up to 1000 [Hz] in the field of automotive applications, but it is no longer accurate enough. Thus, the theory of Bertotti is recommended as a newer approach, in which the iron losses are composed of the three components: hysteresis, eddy-current and excess loss. Here, the excess loss describes that the loss incurred in the magnetizable domains of the material with the migration of block wall and it is still based on empirical factors from curve fitting [4].

$$P_{iron} = P_{hyst} + P_{ed} + P_{excess} \tag{36}$$

The hysteresis loss P_{hyst} corresponds to the area of the static hysteresis loop multiplied by frequency f. For a rectangular shaped hysteresis loop with the coercivity H_c and maximum induction level B_{max} an approximation can be given by first section of (36). The ρ is the material density and k is a dimensionless constant, which is close to 1 for a rectangular shape hysteresis loop. The hysteresis loss is increased by the additional processing allowance K_{bh} considering the influences of the manufacturing technology. For stamped and not finally annealed metal sheets usually K_{bh} =1.5 is used. The eddy-current loss (P_{ed}) which arises by the swirling in the sheet edges is predictable by the conductivity σ and thickness d with a simple approach from the classical Maxwell Equations.

In most cases, the approach does not take displacement current into account because the sheet thickness is so small that the effect is negligible. By the quadratic influence of sheet thickness and the frequency, thin sheets should be used preferably at high supply frequency. For higher frequency eddy-current losses grow to the main contribution to total loss. For a strip material of 0.1 [mm] thickness this is the case at a few kHz and for 0.35 [mm] thickness at a few hundred Hz. The influence of manufacturing technology must be taken into account by an additional processing allowance K_{bh} again. It results from cutting-air of punch and also by tool wear, mostly the stamping burrs. Particularly, thin sheets (d=0.1[mm]) are critical, in which laser- or water jet cutting is preferred. The pollution of the dielectric (pure water) by the burn-up of the baking lacquer layers must be removed by continuous changes of water.

Typical values for the eddy-current additional processing allowance are in punched sheets with K_{bh} =1.5~2.5. The excess loss (P_{excess}) was described by Bertotti for the first time and can be attributed to the magnetic domain structure of the material with sliding Bloch walls. During magnetization, the Bloch walls can not be moved unresistingly, so that an additional energy demand arises. The factor C is the second adjustable factor in measurements and in principle inversely proportional to the number of available magnetizable domains in the considered cross-section. The three loss components can be summarized in (37) in order:

$$P_{fe} = \frac{1}{\rho}\left(4k\,H_c\,B_{\max}\,f\cdot k_{bh} + \frac{\pi^2\sigma\cdot d^2}{6}B_{\max}^2\,f^2\cdot\frac{3}{x}\frac{\sin h(x)-\sin(x)}{\cos h(x)-\cos(x)}k_{bw} + C\,B_{\max}^{1.5}\,f^{1.5}\right) \tag{37}$$

According to the M400-50 material data sheet of ThyssenKrupp, the comparison of the curve fitting with the

measured losses is shown in Fig. 10. The eddy-current loss that occurred in the plate edges by the eddy current is no longer simple relationship as shown in (36).

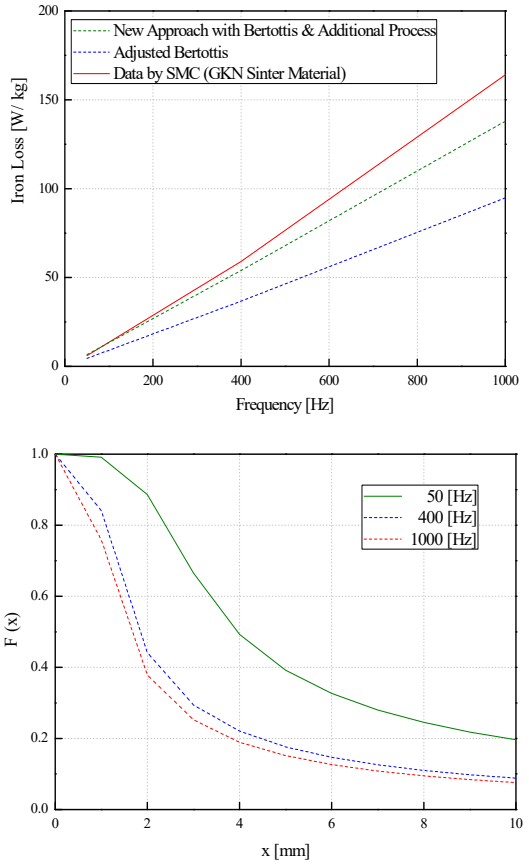

Fig. 10 Losses of M400-50

One of the major problems of PM machines that employ sintered permanent magnets is thermal demagnetization, which is mainly caused by the eddy-current loss of the permanent magnets. This loss results from the time and space harmonics in the air-gap magnetic field produced by slotting effects, as well as the non-sinusoidal stator MMF and phase current waveforms. The calculation of eddy-current loss is simplified considerably by using Poynting's Vector, which is a powerful means of obtaining the total power [5]. The Poynting's Vector is the law of energy conservation and is expreesed by vector multiply between electrical intensity and the magnetic field intensity over the surface of a region. When the problem of magnetic field is expanded in two dimensions, the eddy current loss is calculated with:

$$P_{pm} = \iint_S \frac{J_e^2(r,z)}{\sigma_m} dA = \frac{1}{\sigma_m}\frac{\omega}{2\pi}\int_{r_{im}}^{r_1}\int_{z_0-\frac{l_m}{2}}^{z_0+\frac{l_m}{2}}\int_0^{\frac{2\pi}{\omega}} 2\pi r \cdot J_e^2 \times (r,z,t)\,dt \cdot dz \cdot dr \quad (38)$$

D.Summary

Many application areas demand analytical results for realistic model incorporating the appropriate nonlinear effects. For instance, practical design considerations require that some degree of saturation occurs in the magnetic circuit of the electrical generator. First, it deals with the nonlinearity of saturation overlooked in the previous study using equivalent magnetic circuit. And then, it is compared and evaluated with the results between analytical and numerical calculation. As a result, it shows that the results are in agreement with each other. Moreover, the weight of generator is investigated by kinds of the material and region in terms of the material cost and thermal analysis beforehand. This approach is extended to accurate prediction of power loss for detailed design. It is classified by three kinds of losses; iron loss, copper loss, and eddy-current loss in PM. Here, the iron loss is analyzed through different types of material, and is also considered by three components of losses; hysteresis, classical, and excess loss.

Finally, it will make the detailed design perfect through the design process by equivalent magnetic circuit method and the analyses considering the nonlinearity and losses of the materials selected for cylindrical topology as optimal model.

VI. Shaft Design

Electrical machinery with rotating or linear mass requires a support system that can resist dynamic forces and the resulting vibrations. The excess of such vibrations may be detrimental to the machinery and its support system. Especially, it becomes more and more important for dynamic equipment foundations due to various design criteria and methods and procedures of analysis, design and construction. For stable operation of the equipment foundations, kinetics is an important tool in understanding the motion of objects whether translational, oscillatory, or circular. In case of translating or linear oscillating masses, the behavior of variables such as speed and acceleration (deceleration) must be described by the equations of motion. The reliable design of power transmitting shafts is predicated on three major elements. First, the fatigue characteristics in expected working environment must be established. It can be accomplished from the component of whole-range fatigue test data or approximated using test specimen data [6]. Second, the expected force-iteration history applied the shaft must be obtained or assumed from actual field data and then properly simulated analytically [6]. At last, a reliable analytical model is needed, which reasonably considers both the fatigue characteristics of the shaft and its force history to come to the suitable shaft diameter for the required service reliability and life [6]. Furthermore, bolted joints are treated which have to transit mechanical loads connected with the shaft and which are designed with high duty bolts. The bolts must be designed such that the shaft fulfills its allotted function and withstands the mechanical loads occurring.

A. Fatigue Failure

This fatigue is caused by repeated cycling of the loads. The fatigue strength is dependent on the type of loading (axial, bending, or torsion) and it has resulted in three separate fatigue strengths being defined. In particular, this linear motion is implemented by designing shafts using axial and bending stress

among the three fatigue strengths. The state of stress to be considered is caused by force (torque) transmitted to the shaft, axial forces imparted to the shaft, bending of the shaft due to its weight or loads, and torsion by rotating of shaft. The characteristics of these three basic types or cases are given here: axial strength (σ_a), bending strength (σ_b), and torsion strength (σ_t).

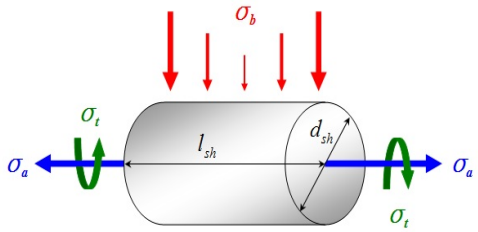

Fig. 11 Three Strengths

$$\sigma_a = \frac{F_{\max}}{A_{rea}} \tag{39}$$

where, A_{area} is cross-section area of the shaft, and F_{max} represents the maximum force considering mechanical load given by (40):

$$F_{\max} = m \cdot a = (m_m + m_l) \cdot \left[\frac{S_t \cdot \omega^2}{2} \right] \tag{40}$$

where, m represents the mass, and it divided by m_m of mover and by m_l of mechanical load.

$$\sigma_b = \frac{32 \cdot M_b}{\pi \cdot d_{sh}^3} \tag{41}$$

It represents as (42) for circular solid [7].

$$\sigma_t = \frac{16 \cdot T_m}{\pi \cdot d_{sh}^3} \tag{42}$$

where, T_m is close to zero, which represents the twisting moment. In this study, the torsional strength is excluded because it has little impact on the shaft due to the linear motion.

The total strength acting on the shaft is expressed by sum of the axial and bending strength.

$$\sigma_{sh} = \sigma_a + \sigma_b \tag{43}$$

$$|\sigma_{sh}| \le \sigma_{al} \tag{44}$$

First systematic study to characterize the fatigue behavior of materials cyclic stress range was conducted by Wöhler [8]. The fatigue failure is often happened in the specific material that is stressed in high cycle. It represents the relationship between the number of repetitions of the stress and its amplitude against the logarithmic scale of cycles to failure. By Wöhler curve, we can find the endurance limit value of selected material; it is marked as σ_{en} in failure cycle 10^6 <N<10^7. The safety factor, ζ, is a ratio of maximum strength to intended loads for the actual item that was designed. The value to use for safety factor is based on designer's judgment or empirical probability.

$$\zeta = \frac{\sigma_{en}}{\sigma_{al}} \rightarrow \sigma_{al} = \frac{\sigma_{en}}{\zeta} \tag{45}$$

Through the earlier analytical calculation, we can attain the total strength acting on the shaft, σ_{sh}. It must not be greater than alternating strength (σ_{al}) by the endurance limit value of selected material and safety factor. Finally, the diameter of shaft is decided by satisfying maximum value below the calculated alternating strength.

B. Summary

The dynamic analysis of single-phase cylindrical topology is performed by using the combination of electric and kinetic equation considering stroke and mechanical load. It provides useful information to analysis the dynamics characteristics of the generator as well as to design of the shaft. Based on this characteristic, an empirical design procedure for shafts with fatigue loadings is presented. The shaft design consists of the prediction of the cause of fatique failure under various operating and loading condition, and the increase of the number of stresses continuously despite of repetition infinite. The shaft diameter is determined by using the axial and bending strength of the selected material by Wöhler curve. In addition, the consideration of the bolt coupling is achieved by influences such as uniform and normal strengths, load, and others for ideal alignment of the shaft, which is made of steel and therefore very rigid, to some intermediate resilient element that can be deformed by relatively small force and decrease the additional load of the shaft. In conclusion, the shaft design and machine element is closely related with the dynamic performances by mechanical load conditions.

VII. Thermal Analysis

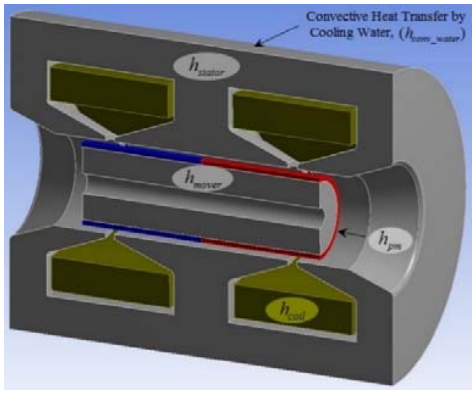

Fig. 12 Cylindrical Topology with Heat Generation

The thermal performance of the generator will determine the power rating of the generator. In order to preserve the optimal conditions ensuring the good operation of the generator, it is imperative to well understand and control the thermal behavior

of the generator. A good understanding needs the ideal design of cooler to ensure the operating temperatures do not exceed the acceptable limits of used materials. As a result, it is obvious that the consideration of thermal characteristic can show the temperature distribution in the generator.

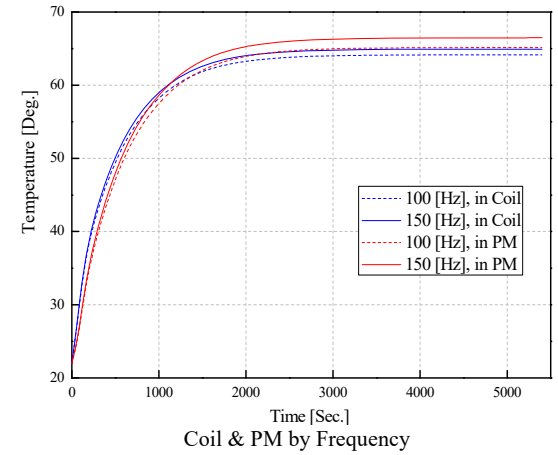

Coil & PM by Frequency

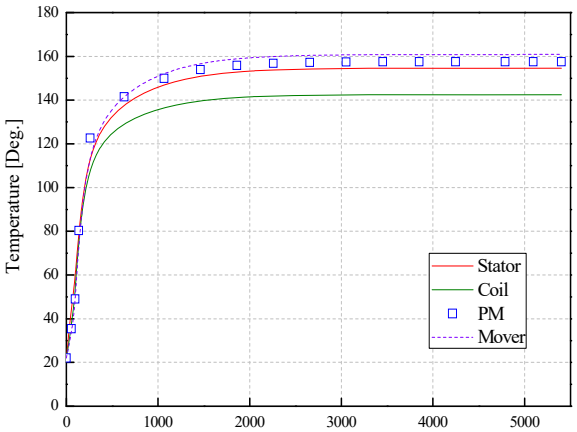

500 [Hz]

Fig. 13 Temperature Distributions

The internal heat coefficients of each region are entered into their losses, namely the input values of each region such as stator, mover, winding, and permanent magnet are decided by the calculated values from losses.

Thermal analysis is very important in generator application to evaluate the effect of temperature in the system. To improve efficiency of the generator, it is necessary to carefully investigate the thermal characteristic in order to determine the best cooling solutions. As a result, it shows that this generator is satisfied with the insulation class *H* in the frequency range from 50 [Hz] to 500 [Hz]. In addition, the temperature distribution of the mover is the highest by comparative estimation in entire regions.

VIII. Assessment

This chapter presents the experiment results to verify the design, and to investigate the performance of the machine as a generator.

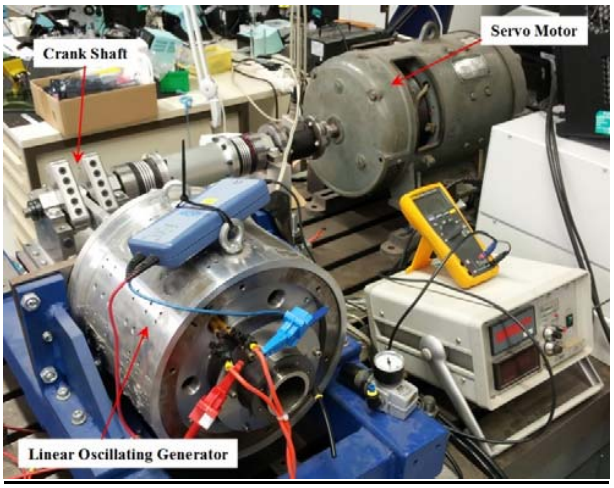

Fig. 14 Test Environment for Measurement

The short-circuit test is carried out with the terminals of the machine short circuited to prevent the machine from saturating from armature reaction. If stand-alone operation is done, the generator is connected to a load and can supply a power and reactive power required under the load.

IX. Conclusion

The objective of this paper is to evaluate a cylindrical linear oscillating generator hybrid electric vehicle. It based on the electrical analysis and structural aspect. The properties of the cylindrical topology are investigated by machine dimensioning with help of the equivalent circuit method considering leakage elements as initial modeling. The reliable design of power transmitting shaft and bolted joints combined with it is performed using fatigue (stress-life) characteristics for stable operation of the equipment foundations. Also, in order to preserve the optimal conditions ensuring the good operation of the generator, it is established to well understand and control the thermal behavior of the generator. The evaluation of the designed and manufactured generator should be achieved by assessment.

The study is concluded by an open-circuit test, short-circuit test, and load test to evaluate the performance of the cylindrical linear oscillating generator. In this measurement, it is assumed that the electrical resistance of the circuit is zero and flux linkage is constant. Each test gives the effective results for more accurate and sustainable operation of the machine.

These results of the study will give elaborate information about the design rules and the performance data of linear oscillating gensets and in parallel tools for the calculation, simulation and the design of linear oscillating machines will be available. It can be useful to more accurate machine design and more accurately prediction of machine performance. The proposed methods allow us to draw a very important design rule, as a result it can be provided to less time of the machine

design and analysis.

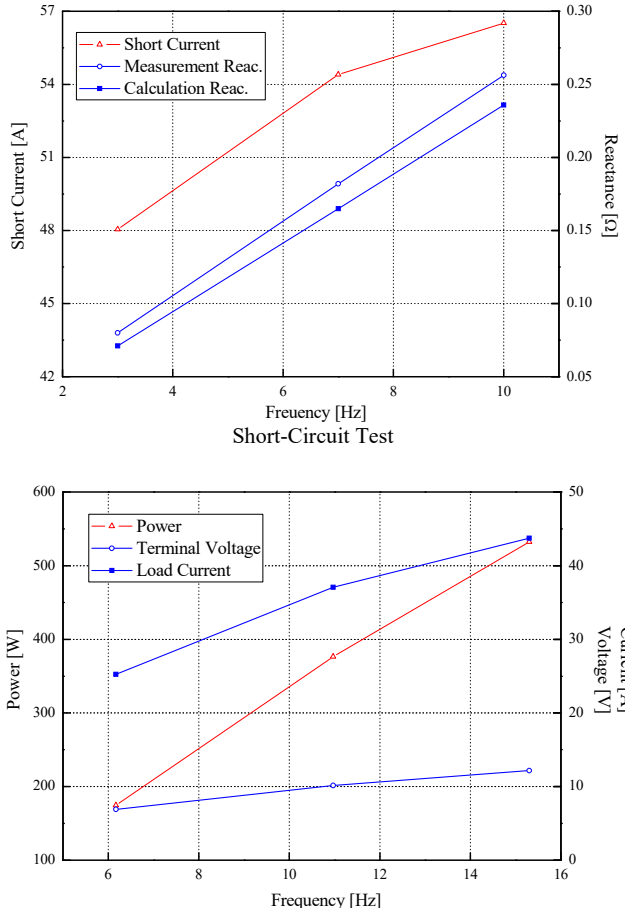

Fig. 15 Cylindrical Topology with Heat Generation

REFERENCES

[1] Sung In Jeong, *Comparative Study of Linear Oscillating Generators*, Dissertation an der Technischen Universität Braunschweig, 2015.
[2] Sun-Ki Hong, Ho-Yong Choi, Jae-Won Lim, Hyo-Jae Lim, Hyun-Kyo Jung, *Analysis of Tubular-type Linear Generator for Free-Piston Engine.*
[3] Dong Liu, *Validation of Eddy Current Loss Models for Permanent Magnet Machines with Concentrated Windings.*
[4] Prof. Dr.-Ing. W.-R. Canders, *Berechnung von Eisenverlusten Physikalisch basierter Ansatz nach Bertottis Theorie*, TB 13-03-03.
[5] Kyoung-Jin Ko, Ji-Hwan Choi, Seok-Myeong Jang, and Jang-Young Choi, *Analysis of eddy current losses in cylindrical linear oscillatory actuator with Halbach permanent magnet array mover*, Journal of Applied Physics 111, 07B547 (2012); doi: 10.1063/1.3678316.
[6] Stuart H. Loewenthal, *Factors That Affect the Fatigue Strength of Power Transmission Shafting and Their Impact on Design*, NASA Technical Memorandum 83608.
[7] *TORSION of SHAFTS*, Department of Chemical Engineering Strength of Materials for Chemical Engineers.
[8] V. B. Bhandari, *Design of Machine Elements*

Sungin Jeong received B.S. and M.S. degrees in Electrical Engineering from Dongguk and Hanyang University, South Korea, respectively. And then he was responsible for the development of electrical machine and its drive at Samsung Heavy Industry, Samsung Electronics, and Daewoo Electronics, in order. After he received Dr. Ing. degree from Technical University Braunschweig, Germany. He is in the Daelim Motor, South Korea. His research and development field and interest included design, analysis and drive of electric machine for personal motilities.